J Mater Sci: Mater Med (2016) 27:26
DOI 10.1007/s10856-015-5635-8

DELIVERY SYSTEMS

Original Research

Biocompatible polymers coated on carboxylated nanotubes functionalized with betulinic acid for effective drug delivery

Julia M. Tan[1] · Govindarajan Karthivashan[2] · Shafinaz Abd Gani[2] · Sharida Fakurazi[2,3] · Mohd Zobir Hussein[1]

Received: 13 August 2015 / Accepted: 23 November 2015 / Published online: 24 December 2015

Abstract Chemically functionalized carbon nanotubes are highly suitable and promising materials for potential biomedical applications like drug delivery due to their distinct physico-chemical characteristics and unique architecture. However, they are often associated with problems like insoluble in physiological environment and cytotoxicity issue due to impurities and catalyst residues contained in the nanotubes. On the other hand, surface coating agents play an essential role in preventing the nanoparticles from excessive agglomeration as well as providing good water dispersibility by replacing the hydrophobic surfaces of nanoparticles with hydrophilic moieties. Therefore, we have prepared four types of biopolymer-coated single walled carbon nanotubes systems functionalized with anticancer drug, betulinic acid in the presence of Tween 20, Tween 80, polyethylene glycol and chitosan as a comparative study. The Fourier transform infrared spectroscopy studies confirm the bonding of the coating molecules with the SWBA and these results were further supported by Raman spectroscopy. All chemically coated samples were found to release the drug in a slow, sustained and prolonged fashion compared to the uncoated ones, with the best fit to pseudo-second order kinetic model. The cytotoxic effects of the synthesized samples were evaluated in mouse embryonic fibroblast cells (3T3) at 24, 48 and 72 h. The in vitro results reveal that the cytotoxicity of the samples were dependent upon the drug release profiles as well as the chemical components of the surface coating agents. In general, the initial burst, drug release pattern and cytotoxicity could be well-controlled by carefully selecting the desired materials to suit different therapeutic applications.

✉ Mohd Zobir Hussein
mzobir@upm.edu.my

Julia M. Tan
julia.tanmh@gmail.com

[1] Materials Synthesis and Characterization Laboratory, Institute of Advanced Technology (ITMA), Universiti Putra Malaysia, 43400 Serdang, Selangor, Malaysia

[2] Laboratory of Vaccine and Immunotherapeutics, Institute of Bioscience (IBS), Universiti Putra Malaysia, 43400 Serdang, Selangor, Malaysia

[3] Department of Human Anatomy, Faculty of Medicine and Health Sciences, Universiti Putra Malaysia, 43400 Serdang, Selangor, Malaysia

1 Introduction

In recent years, chemically functionalized carbon nanotubes (CNT) have been studied intensively for drug delivery applications [1] because of their high cargo loading [2], non-immunogenic property [3], good stability in aqueous medium [4] and most importantly, they are able to cross the cell barriers without the use of external targeting moieties [5]. Although these advantages offered by chemically modified CNT are promising, recent findings suggested that functionalization (e.g., carboxyl and hydroxyl groups) to the sidewall of CNT leads to a higher degree of in vitro cytotoxicity when compared to non-functionalized CNT [6, 7]. Hence, in order to mask the cytotoxic effect of CNT, several strategies are currently being employed to coat CNT with various types of surfactants [8] or polymers [4, 9] and render them more biocompatible. The coating on the CNT surface is an imperative step to shield the nanotubes from the surrounding environment so that their pharmacokinetic profiles (i.e., stability, cytotoxicity, solubility and prolonged release in the circulation half-life) can be significantly

enhanced and at the same time, protect the drug from rapid enzymatic degradation.

In our previous work [10], we have synthesized and studied the in vitro cytotoxic effect of carboxylated single walled carbon nanotubes (SWCNT-COOH)-based drug delivery system for anticancer drug, betulinic acid (3β, hydroxy-lup-20(29)-en-28-oic acid, BA). Based on our published cytotoxicity assay, the conjugate (SWBA) exhibited significant anticancer activity of BA against human lung A549 cells when compared to human liver HepG2 cells, with approximately 15 wt% of loaded BA in the nanotubes. However, the conjugate was also seen to exert cytotoxicity in healthy fibroblast cell line (3T3) when the cells were exposed to concentration of 50 μg/mL, causing more than 50 % reduction in cell viability after 72 h of treatment. The basis of this reduction could be possibly attributed to the grafted functional groups such as –COOH, –C=O or –OH [11] and the inherent toxic effect of BA itself [12]. To further improve the biocompatibility of the said conjugate for a safe and effective drug delivery without compromising the active ingredients of BA, we have therefore, proposed these four coating biomaterials, namely Tween 20 (T20), Tween 80 (T80), polyethylene glycol (PEG) and chitosan (CHI) as a comparative study in order to evaluate the cytotoxic effects of SWBA interactions with 3T3 cells.

Surfactants, depending on their polar functional groups, can be classified into four major categories: anionic, cationic, nonionic and amphoteric. Among them, nonionic surfactants are known to be less irritating as most of them do not denature proteins and they generally have a lower toxic effect [13]. Furthermore, they have no electrostatic interactions with CNT and the steric hindrance caused by the chemical moieties prevents the agglomeration of nanotubes [14]. Tween surfactants (e.g. T20 and T80) are being widely utilized as stabilizers for preventing aggregation in protein formulations [15] as well as emulsifiers in foods and cosmetics. These molecules are nonionic polysorbates, where each molecules having a group of long polyoxyethylene glycol chain as the hydrophilic head and a fatty acid ester moiety as the hydrophobic alkyl tail. The only difference between them is that, T20 contains primarily lauric acid while T80 has mainly oleic acid. This difference is essentially crucial, especially in a biological study because T20 and T80 demonstrated different levels of hemolytic activity depending on the length of the polyoxyethylene glycol chain [16]. Although Tween members are routinely being used as mild washing agent in biomedical laboratory to reduce nonspecific binding of antibodies or to remove unbound moieties, but very little has been reported on how these differences can actually affect the drug release and cytotoxicity of a drug delivery system. For this purpose, we have chosen T20 and T80 as the nonionic surface coating and their chemical structures are shown in Fig. 1.

PEG, a viscous liquid of hydrophilic polymer with molecular weight 300 (as shown in Fig. 1), has been selected as the surface coating polymer since PEG is extensively used as co-solvent or vehicle in pharmaceutical preparations like coatings of pill, bases of water-soluble ointment and ingredients of suppository. In general, PEG is known to have a very low order of acute toxicity and it reduces the tendency of drugs to aggregate in vivo, as a result of the steric hindrance [17].

CHI is a natural biopolymer that has gained a great deal of attention as an efficient drug delivery vehicle due to its excellent biocompatibility, biodegradability, antibacterial effect and drug loading and release capacity [18, 19]. Moreover, CHI has both $–NH_2$ and –OH functional groups that can further encourage hydrogen bonding interactions with the COOH groups of carboxylated SWCNT and BA. The chemical structure of CHI is presented in Fig. 1.

The main objective of this work was to study the coating effects of four bioactive materials (T20, T80, PEG, and CHI) on a real time drug release mode of the developed SWBA as well as their in vitro cytotoxicity to 3T3 cells as determined by 3-(4,5-dimethylthiazol-2-yl)-2,5-diphenyltetrazolium bromide (MTT) assay. In addition, the physicochemical property and surface morphology of the coated SWBA nanocomposites were also investigated.

2 Experimental section

2.1 Chemicals

Chemical vapour deposition-fabricated SWCNT-COOH (purity >90 w/w%; COOH functional content 2.73 w/w% and diameter 1–2 nm) was sourced from Chengdu Organic Chemicals Co., Ltd. (Chengdu, China) and used without further purification. Pure BA ($C_{30}H_{48}O_3$, molecular weight 456.70) of ≥98 % purity, T20 ($C_{58}H_{114}O_{26}$, polyoxyethylenesorbitan monolaurate), T80 ($C_{64}H_{124}O_{26}$, polyoxyethylenesorbitan monooleate) and CHI (low molecular weight, deacetylation 75–85 %) were purchased from Sigma-Aldrich (Saint Louis, USA). PEG (average molecular weight 300) was purchased from Acros Organics (Geel, Belgium). Methanol (99.8 % purity), solvent for BA and aqueous acetic acid solution (99.8 % purity), solvent for CHI was obtained from HmbG Chemicals (Hamburg, Germany). 3T3 cells were bought from American Tissue Culture Collection (ATCC). 3-(4,5-dimethylthiazol-2-yl)-2,5-diphenyltetrazolium bromide (MTT) was purchased from PhytoTechnology Laboratories (Kansas, USA). All chemicals used in this study were analytical reagent grade and used as received.

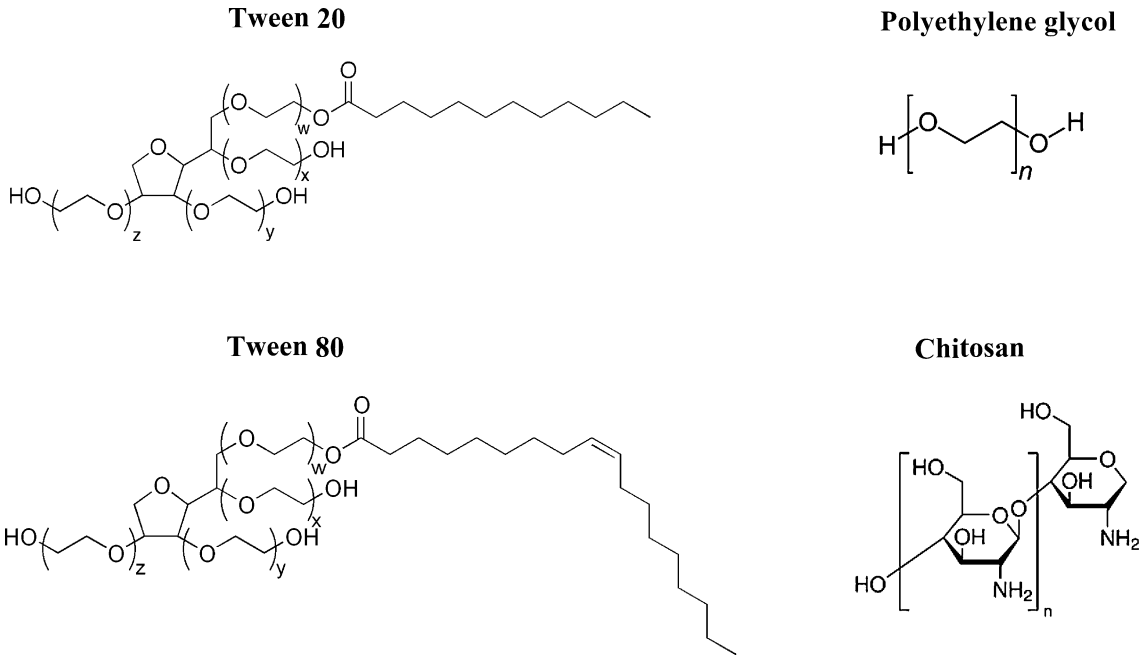

Fig. 1 Molecular structure of Tween 20 and Tween 80, where w + x + y + z = 20; polyethylene glycol and chitosan

2.2 Characterization

Infrared spectra were recorded on a Thermo Nicolet Nexus Smart Orbit FTIR (Vernon Hills, USA) over the range of 4000–500 cm^{-1}. Raman scattering studies using laser beam of wavelength 532 nm were carried out at room temperature using a Raman spectrometer WITec UHTS 300 (Germany). Nanotubes samples were investigated using a HR TEM with FEI Tecnai G2 (Oregon, USA) at magnifications of 400 kx. Surface morphologies of the samples were analyzed by a FESEM, Hitachi UHR SU8030 (Tokyo, Japan) with an acceleration voltage of 10 kV and magnifications of 100 kx. A ultraviolet–visible (UV–Vis) spectrophotometer Perkin Elmer Lambda 35 (Boston, USA) was used to detect the BA release amount in PBS (pH 7.4) at 210 nm. Thermogravimetric analysis (TGA) was performed with a TA Instruments, model Q500 (New Castle, DE) and the samples were heated from room temperature up to 1000 °C with a heating rate of 10 °C/min under a nitrogen purge of 40 mL/min.

2.3 Synthesis of betulinic acid-loaded single walled carbon nanotubes

BA-loaded SWCNT (SWBA) was synthesized via non-covalent approach by adding carboxylated SWCNT (400 mg) as the starting material in a solution of BA (50 mg dissolved in 400 mL of methanol) [10]. The nanotubes suspension was then sonicated in a water bath for 1 h and the pH of the suspension was slowly adjusted to 4.0. Subsequently, the mixture was left to proceed by vigorously stirring for about 22 h under a dark, chemical fume hood at room temperature. The resulting product, SWBA was obtained after three cycles of centrifugation and washing with methanol, followed by deionized water in order to remove excessive BA. Finally, the product was allowed to dry completely in an oven at 60 °C.

2.4 Synthesis of biopolymer-coated SWBA nanocomposites

To synthesize Tween-coated SWBA nanocomposites, 100 mg of SWBA was added to 100 mL of T20 or T80 (1 % v/v) dissolved solution and reacted with continuously stirring for 24 h [20]. Subsequently, the mixtures were then collected and subjected to further centrifugation and excessive washing with deionized water three times. Finally, the resulting products were dried overnight in an oven to obtain SWBA-T20 or SWBA-T80 nanocomposites.

PEG-coated SWBA sample was prepared as previously reported, with slight modification [21]. Briefly, the synthesized SWBA (100 mg) was mixed with 1 % (v/v) PEG solution and stirred at room temperature for 24 h. The reaction mixture was extracted repeatedly by centrifugation and rinsing with deionized water, and then dried in a vacuum oven to obtain SWBA-PEG. Similarly, coated-SWBA by low molecular weight CHI was prepared under the same condition using 0.5 % (v/v) CHI as the coating agent and the product was denoted as SWBA-CHI.

To determine the wt% of the coating agents, a set of 4 samples without drug was prepared under the same coating

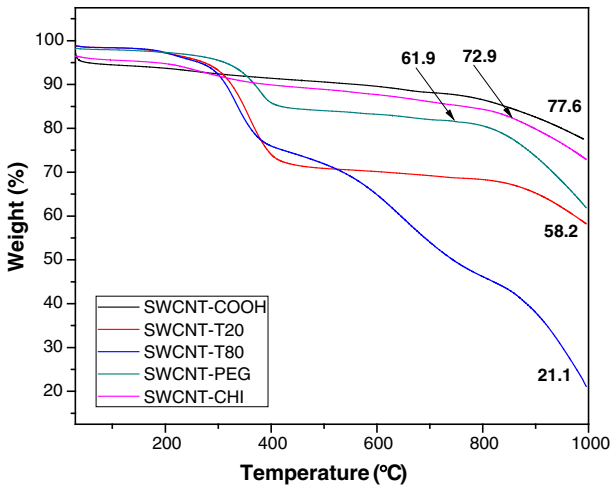

Fig. 2 TGA weight loss curves for coated samples without drug

Table 1 TGA data of the coated samples without the anticancer drug, BA

Samples	Residue (wt%)	[a]Coating (wt%)
SWCNT-COOH (uncoated)	77.6	–
SWCNT-T20	58.2	19.3
SWCNT-T80	21.1	56.4
SWCNT-PEG	61.9	15.7
SWCNT-CHI	72.9	4.6

[a] Estimated value from TGA analysis based on the wt% difference between the uncoated and coated samples

condition as mentioned above. The samples were denoted as SWCNT-T20, SWCNT-T80, SWCNT-PEG, and SWCNT-CHI. The polymer content of the coated SWCNT was determined by TGA (Fig. 2) and the coating percentage of each biopolymer is presented in Table 1.

2.5 Drug release and kinetic studies of biopolymer-coated SWBA nanocomposites

The in vitro release of BA in PBS solution at pH 7.4 (simulating human body physiological condition) was analyzed using a UV–Vis spectrophotometer at λ_{max} of 210 nm. Briefly, 1 mg of the sample was added to the releasing PBS buffer solution (3.5 mL) and the accumulated release amount of BA was recorded at preset time intervals.

To examine the release mechanism of BA, in vitro drug release data were fitted into four mathematical kinetic models, i.e., zero order, first order, second order and Higuchi model. The zero order rate describes the system where the drug release rate is independent on its concentration. In first order release kinetic, the drug release rate is concentration dependent. For a second order reaction, the reaction rate is proportional to the square of the concentration of one of the reactants. Higuchi's model describes the release of drugs from an insoluble polymeric matrix as a square root of time-dependent process based on Fickian diffusion release behaviour.

2.6 Cell line and cell culture

Cytotoxicity experiment was performed on 3T3 cell line (derived from mouse embryonic fibroblasts) and maintained as a monolayer culture in RPMI 1640D medium supplemented with 10 % fetal bovine serum, 15 mmol/L L-glutamine and 1 % penicillin (100 units/mL)/streptomycin (100 µg/mL). The cells were then grown in a humidified atmosphere containing 5 % CO_2 at 37 °C. When confluent (approximately 80 %), the cell line was transferred and subcultured in a new culture flask for seeding and treatment purposes. Stock solutions (10 mg/mL) containing the biopolymer-coated nanocomposites were freshly prepared in PBS solution and diluted serially to the desired concentrations of 0 µg/mL (control) to 100 µg/mL.

2.7 Cytotoxicity assay

Cytotoxicity of the biopolymer-coated nanocomposites was determined by quantification of cell viability via MTT assay. 3T3 cells were seeded ($1x10^5$ cells/well) in 96-well plate and incubated at 37 °C (5 % CO_2 and 95 % air) for 24 h to allow cell attachment. Subsequently, the cells were exposed to different concentrations for 24, 48, and 72 h. Following incubation, 20 µL MTT (5 mg/mL in PBS) was added to each well and the plate was incubated for 3 h. Thereafter, the excess MTT was removed and 150 µL of dimethylsulfoxide was added to dissolve the formazan crystals formed in the assay. The cell viability was measured with a microplate reader model EL 800X (Winooski, VT) at 570 nm with 630 nm as reference wavelength. Experiments were performed in triplicate and the results were expressed as mean $\pm$ standard deviation (SD).

3 Results and discussion

3.1 Chemical structures of the biopolymer-coated SWBA nanocomposites

The chemical structures of SWCNT-COOH, BA and their nanohybrid (SWBA) have been discussed in our previous paper and hence, the emphasis is focused on the coating agents used in the present study. Figure 3 shows the Fourier transform infrared (FTIR) spectra of the SWBA-coated nanocomposites and their constituents. Based on Fig. 3a, the spectrum of pure T20 demonstrates strong

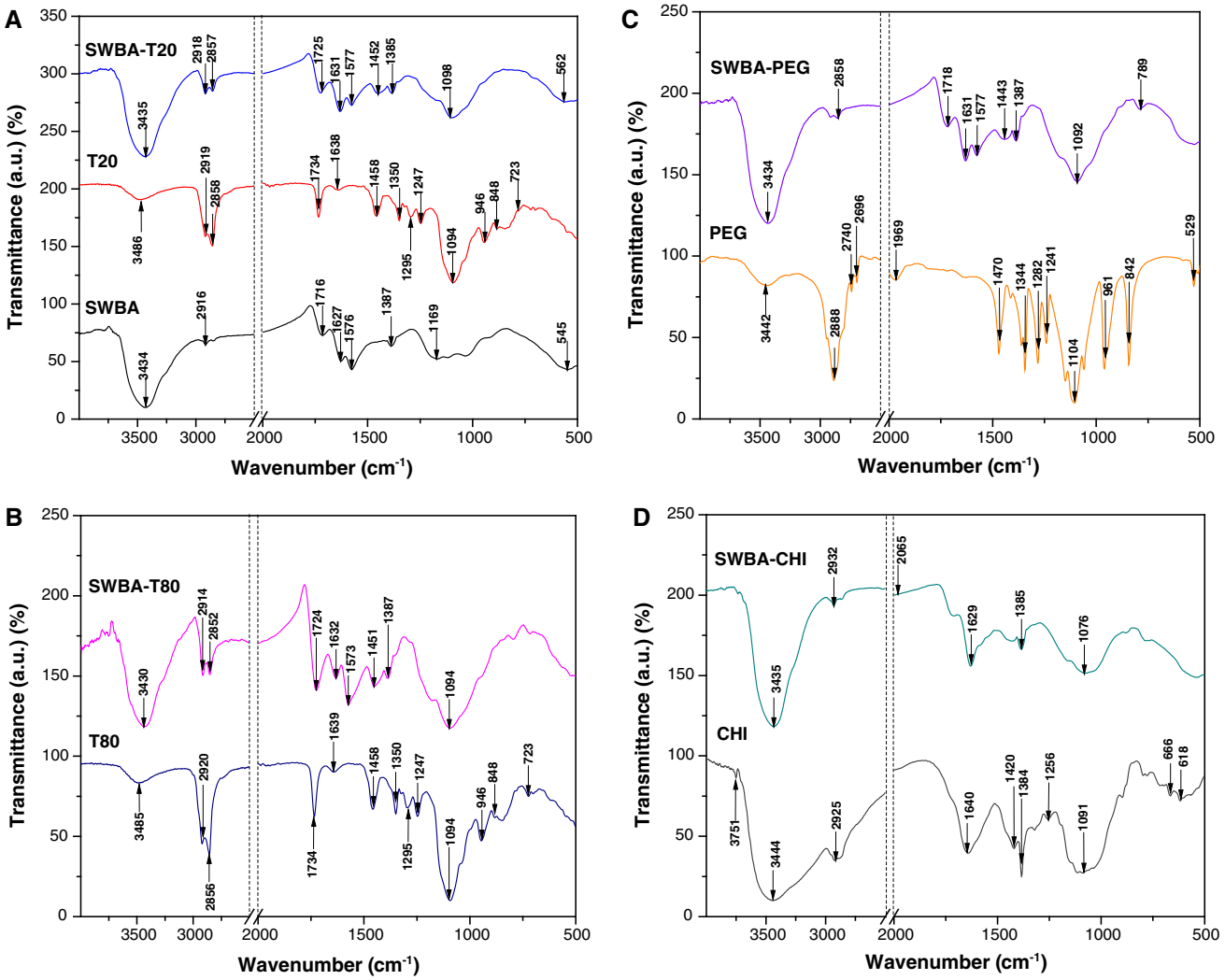

Fig. 3 FTIR spectra of **a** T20 coated SWBA, **b** T80 coated SWBA, **c** PEG coated SWBA, and **d** CHI coated SWBA

bands at 2919 and 2858 cm^{-1} due to the stretching of asymmetrical and symmetrical $–CH_2$ bonds [22]. The characteristic peaks at 1458 and 1350 cm^{-1} are assigned to the asymmetrical and symmetrical bending vibrations of $–CH_3$ [23]. The other bands centered at 3486 and 1734 cm^{-1} are due to O–H stretching vibrations and C=O stretching of the ester group [24], respectively. Therefore, the existence of these peaks observed in SWBA-T20 indicate that the T20 was coated on the surface of SWBA. The chemical structure of T80 is similar to that of T20, with the characteristic absorption bands occurred in the wavenumber region of 3486, 2920, 2856, 1734, 1458 and 1350 cm^{-1} (Fig. 3b), correspond to O–H, $–CH_2$, C=O, and $–CH_3$, respectively. It can be significantly seen that the relative intensity of these peaks assigned to the respective functional groups are also appeared in SWBA-T80.

The FTIR spectra of the pure PEG and the PEG-coated SWBA nanocomposites are presented in Fig. 3c. For the PEG-coated SWBA nanocomposites, an intense absorption band was observed at 3434 cm^{-1} which is the characteristic of the O–H stretching mode of the carboxylic acid groups for SWCNTs and the hydroxyl groups of PEG chains. The IR bands at 2858 cm^{-1} is due to the C–H stretching whereas 1443 and 1387 cm^{-1} are due to the C-H bending vibrations of PEG [25] in the sample of SWBA-PEG. The bands correspond to the O–H, C–H and C–O–H functional groups are the strong evidence to show that the synthesized SWBA nanocomposites surface has been coated with PEG.

For the case of CHI-coated SWBA nanocomposites, it has been observed that there is a slight shift in the absorption bands obtained when compared to the pure CHI (Fig. 3d). The band occurred at 3435 cm^{-1} represents the stretching vibrations of O–H, the band at 1629 cm^{-1} is assigned to the stretching vibrations of acetylated amino group of chitin [26], the peak at 1385 cm^{-1} is attributed to

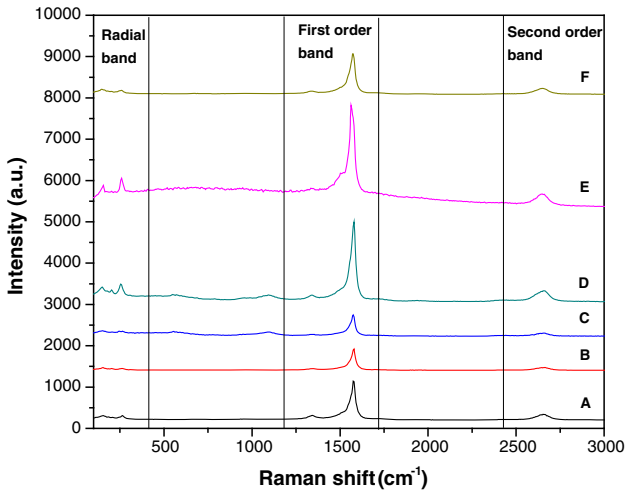

Fig. 4 Raman spectra for (*a*) carboxylated SWCNT, (*b*) SWBA, (*c*) SWBA-T20, (*d*) SWBA-T80, (*e*) SWBA-PEG, and (*f*) SWBA-CHI

the vibrations of C–N stretching of the free primary amino group at C_2 position of glucosamine [27] and the strong band at 1076 cm^{-1} is due to the C–O–C bond in six member ring [28], which confirms the presence of CHI.

There are four important characteristic peaks to be observed in the Raman spectra of the SWCNT and their nanocomposites, as shown in Fig. 4. The presence of radial breathing mode (RBM) in the range of 100–300 cm^{-1}, second peak near 1342 cm^{-1} represents the D-band, third peak at 1575 cm^{-1} represents the G-band and the fourth peak centered at 2654 cm^{-1} indicates the presence of the 2D-band in SWCNT. RBM is a low vibrational mode corresponding to the radial direction of the carbon atoms in CNT and is not observed in other carbon materials [29]. The D-band is typically assigned to the disorder and surface defects in the sidewall structure of carbon systems [30]. G-band is due to the stretching vibrations of the C–C bonds in planar sheets for most graphitic materials [31], whereas 2D-band is the overtone mode of the D-band.

Typically, the extent of defect density in SWCNT can be determined by a quantitative measurement from the intensity ratio of D and G-bands (I_D/I_G). The positions of D and G-bands as well as the I_D/I_G ratio for all samples have been obtained from Fig. 4, and their respective values are listed in Table 2. It was noted that the I_D/I_G ratio of SWBA is substantially higher than that of the starting material, SWCNT-COOH, used in the present study. However, in the case of biopolymer-coated SWBA nanocomposites, the I_D/I_G ratios decreased significantly after coating treatment with the lowest value observed for SWBA-T80. As this ratio is an assessment of defect density in SWCNT, it indicates that T80 has the best coverage on SWBA (Table 1 shows the content concentration of T80 is about 56.4 wt% as estimated by TGA) when compared to others. As a result, fewer surface defects are detected in SWBA-T80. In addition to that, the position of D and G-bands of all SWCNT samples do not change much, suggesting that the structural integrity of the SWCNT is preserved under all these various surface functionalization steps (drug attachment and coating process).

3.2 Morphological studies of the SWBA nanocomposites

High resolution transmission electron microscope (HR TEM) and field emission electron microscope (FESEM) techniques have been used in complementary in order to characterize SWCNT-COOH, BA-loaded SWCNT and biopolymer-coated SWBA nanocomposites as demonstrated in Figs. 5 and 6, respectively. According to the HR TEM micrograph in Fig. 5a, it can be seen that the carboxylated nanotubes exhibit smooth external surface without deposition of amorphous carbon and/or noticeable surface defects. A dark spot was detected after functionalization with BA, as shown by the white arrow in Fig. 5b, and this could possibly be due to the presence of BA molecule being encapsulated in the nanotubes. Similar observation was recently reported by a group of researchers in Poland for their in vivo study on CNT-based haemostatic dressing filled with cisplatin, an anticancer drug [32]. They reported that several tiny dark spots corresponding to the presence of cisplatin were observed on the surface and/or encapsulated in between the nanotubes using HR TEM.

Figure 6 shows the FESEM micrographs of SWCNT-COOH and biopolymer-coated SWBA nanocomposites. In comparison to carboxylated SWCNT (Fig. 6a), the tubular structures of all coated nanotubes (Fig. 6b–e) do not sustain significant damage after the coating process. This

Table 2 Raman shifts for SWCNT-COOH, SWBA and the biopolymer-coated SWBA nanocomposites

Sample	Position of D-band (cm^{-1})	Position of G-band (cm^{-1})	I_D/I_G
SWCNT-COOH	1342	1575	0.273
SWBA	1346	1579	0.339
SWBA-T20	1346	1575	0.331
SWBA-T80	1338	1579	0.188
SWBA-PEG	1334	1563	0.271
SWBA-CHI	1334	1575	0.235

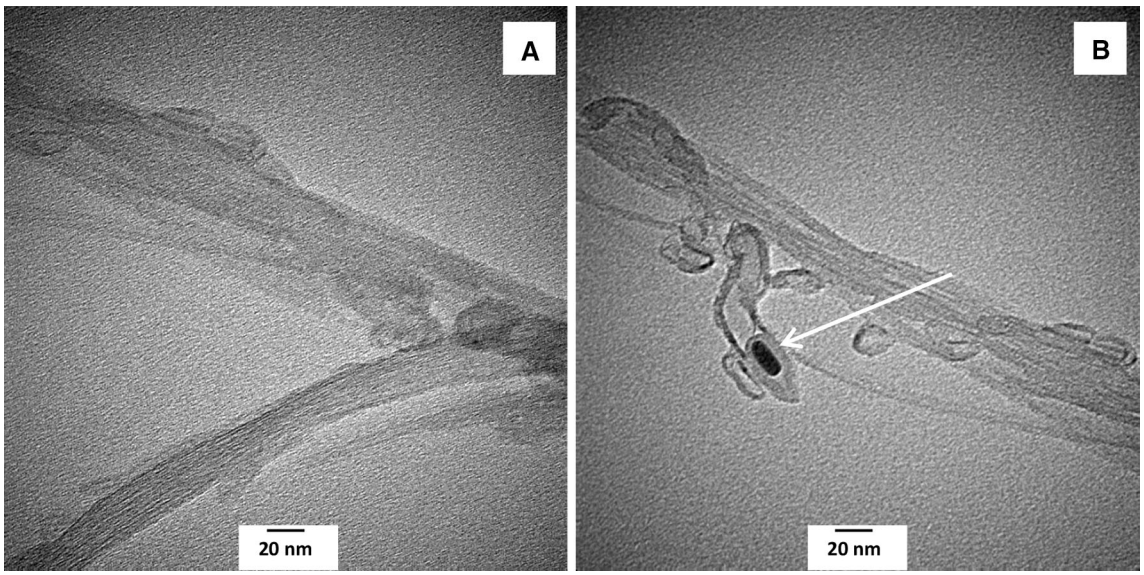

Fig. 5 HR TEM images of the **a** carboxylated SWCNT and **b** BA-loaded SWCNT. The *arrow* indicates possible location of BA molecule being encapsulated in the nanotubes

morphological observation is in good agreement with the Raman spectra shown in Fig. 4 where no significant D and G-band shifts were observed for all coated samples.

3.3 Drug release and kinetic studies of the biopolymer-coated SWBA nanocomposites

Previously, we reported that the rapid burst release of BA was observed in the first 20 min and then followed by a slow release up to 1400 min. Since the burst release is often regarded as the common phenomenon associated with the surface-bound drugs [33], we have therefore decided to work on the encapsulation method to reduce the initial burst by coating the system separately with different surface coating agents. The release profiles of BA from the uncoated and coated SWBA nanocomposites were examined in neutral environment (pH 7.4) on a real time drug release basis (Fig. 7). There are significant differences to be observed in the initial drug release stage as a result of the surface coating treatment (Fig. 7a). The release of BA from uncoated SWBA during the first 20 min was approximately 73 %, and the extent of release was reduced dramatically to about 10–30 % with the presence of coating agents. This is because the polymer formed an additional layer to encapsulate the system, making the drug inaccessible for instant release [34], thereby the release rate of BA was reduced. After 1400 min, the released BA from uncoated sample was nearly 89 %, whereas the coated samples demonstrated slow and sustained release fashion during the following days. After 3500 min, release of BA from coated samples could still be observed.

Figure 7b illustrates the drug release behaviour of BA from each biopolymer-coated system follows the sequence of SWBA-PEG > SWBA-T80 > SWBA-CHI > SWBA-T20. The higher release of BA from PEG-coated SWBA may be attributed to the polymer's major affinity for water molecules [35], which leads to higher solubility in the release medium. The different release pattern of BA from Tween-coated samples was found to be dependent upon the chemical structure of these surfactants. In particular, sample coated by T80 showed higher release rate (~70 %) than T20 (~41 %) ones. This observation can be interrelated with the hydrophilic-lipophilic balance (HLB) values characterized by these surface coating agents as listed in Table 3. T80 with a HLB value of 15.0 is most lipophilic in nature compared with T20, which has a value of 16.7, and hence, the solubility of lipophilic molecule like BA increases as the hydrophobic chain length of surfactant increases. As a result, BA has the tendency to diffuse into the layer of T80 coating more rapidly in comparison with that of T20 coating, and causes an increment in the concentration of released BA. Besides, the molecular chains of the Tween series in the drug-loaded system would undergo different extent of chain relaxation due to the electrostatic repulsion from the ionized hydrophilic carboxyl groups when they were placed in the medium at pH 7.4 [36]. In the case of CHI-coated SWBA, the incomplete release of BA occurred by diffusion through the polymer backbone absorbed with water instead of the degradation of the polymer itself [37]. The BA molecules initially diffused from the surface of CNT, then into the CHI layer which leads to the subsequent swelling of the polymer causing a

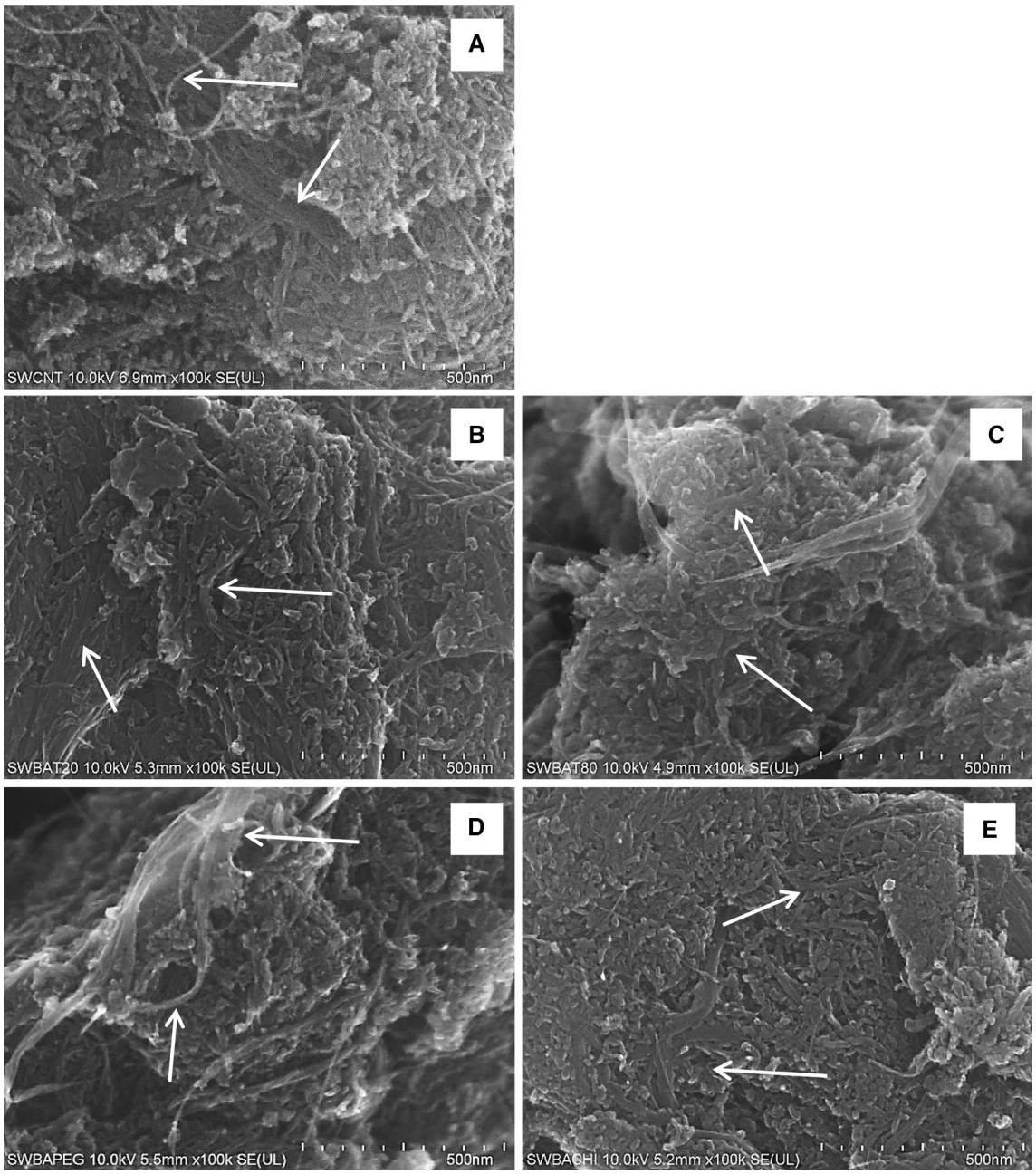

Fig. 6 FESEM images of the **a** carboxylated SWCNT and biopolymer-coated SWBA nanocomposites: **b** T20 coated SWBA, **c** T80 coated SWBA, **d** PEG coated SWBA, and **e** CHI coated SWBA. The *arrows* indicate the tubular structures of the nanotubes

constant slow release before being released into the medium. The in vitro release experiments show that the drug release behaviour can be altered by carefully choosing the desired polymer as the surface coating agent to suit different biomedical applications (e.g., initial burst for anesthetic purpose or slow, sustained release for anticancer treatment).

In order to design a more effective drug delivery system for therapeutic application, it is essential to determine the drug release profiles using model-dependent methods, like zero order, pseudo-first order, pseudo-second order, and Higuchi models based on different mathematical functions [39, 40]. By fitting the BA release data obtained from Fig. 7 into the respective equations of the four kinetic models, the linear fits of curves of different release behaviours are summarized in Table 4. The calculated correlation coefficient (R^2) values of the release data reveal that the release kinetic of all samples fitted well to the pseudo-second order kinetic behaviour. This indicates that the overall reaction is dependent upon the ion exchange

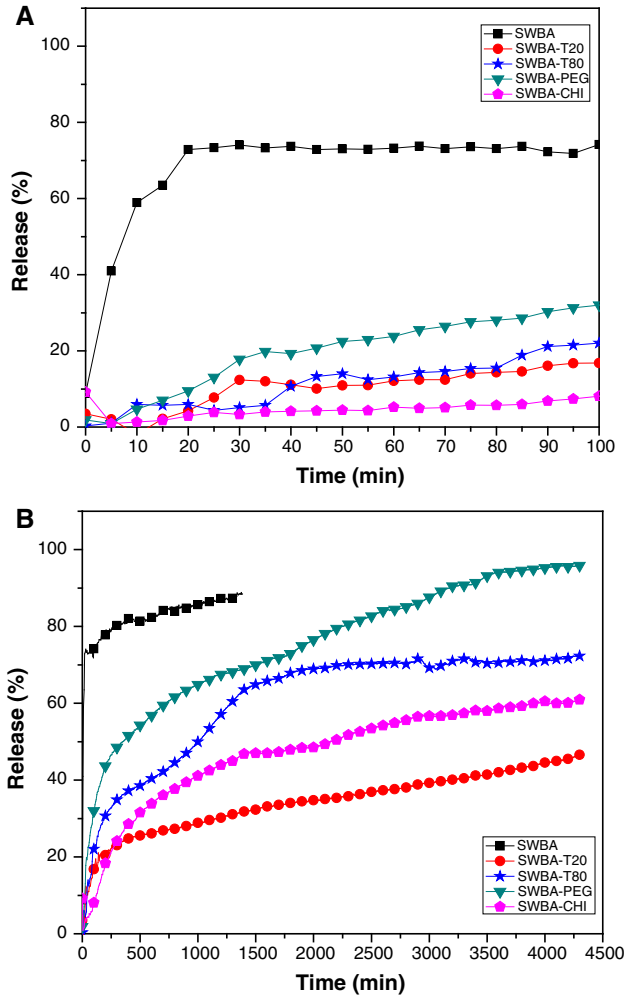

Fig. 7 Comparative drug release kinetics of BA from biopolymer-coated SWBA nanocomposites into PBS solution at pH 7.4. **a** Burst release; **b** slow and sustained release

between the drug molecules and the release medium (PBS contains anions like $H_2PO_4^-$, HPO_4^{2-}, Cl^-, etc.) at the time of release and that released at equilibrium [41].

3.4 Cytotoxicity assay

The cytotoxicity characteristics of the biopolymer-coated SWBA nanocomposites were determined using a standard MTT cell proliferation assay kit with 3T3 cells, which is an important step towards realizing such material as drug delivery system. As mentioned earlier in the introduction, there was a significant reduction of viable cells (>50 %) when the SWBA concentration exceeded 50 μg/mL. In the present study, after 72 h incubation with the biopolymer-coated SWBA, all samples showed major improvement with satisfactory biocompatibility where the proliferation of 3T3 cells remained above 80 %, even at a concentration of 100 μg/mL (Fig. 8). These in vitro findings clearly indicate that SWBA when wrapped with biocompatible surface coating agents, the cytotoxic effect of CNT will be greatly reduced which is consistent with previous reports [42, 43]. However, this is not the case for PEG-coated SWBA where a slightly higher cytotoxicity was observed in the 3T3 cell line as shown in Fig. 8c. It was noted that after 72 h of exposure at concentrations more than 50 μg/mL, the viability of 3T3 cells was reduced to about 50 %. This could be due to the low molecular weight of PEG (average molecular weight 300) used in the study. According to the literature [44, 45], these low-molecular-weight glycols (i.e., monomer, dimer, and trimer) are considered as toxic substances. On the other hand, even though most PEG are widely reported to be non-toxic, the consequences of the impurities (e.g., ethylene oxide, fatty

Table 3 Physical parameters of Tween series

Product name	Molecular formula	Molecular weight (g mol^{-1})	HLB	Hydrophobic group
Tween 20	$C_{58}H_{114}O_{26}$	1228	16.7	Laurate (C12)
Tween 80	$C_{64}H_{124}O_{26}$	1310	15.0	Oleate (C18) (double bond)

Adapted from [38] with permission

Table 4 The correlation coefficients (R^2) obtained by fitting the BA release data from biocompatible polymer-coated SWBA nanocomposites into PBS solution at pH 7.4

Sample	Drug release (%)	R^2			
		Zero order	Pseudo-first order	Pseudo-second order	Higuchi model
SWBA	89	0.4899	0.8817	0.9992	0.7054
SWBA-T20	47	0.9140	0.9787	0.9777	0.9716
SWBA-T80	73	0.6965	0.9332	0.9936	0.8535
SWBA-PEG	96	0.8709	0.8629	0.9860	0.9606
SWBA-CHI	61	0.8139	0.9547	0.9946	0.9373

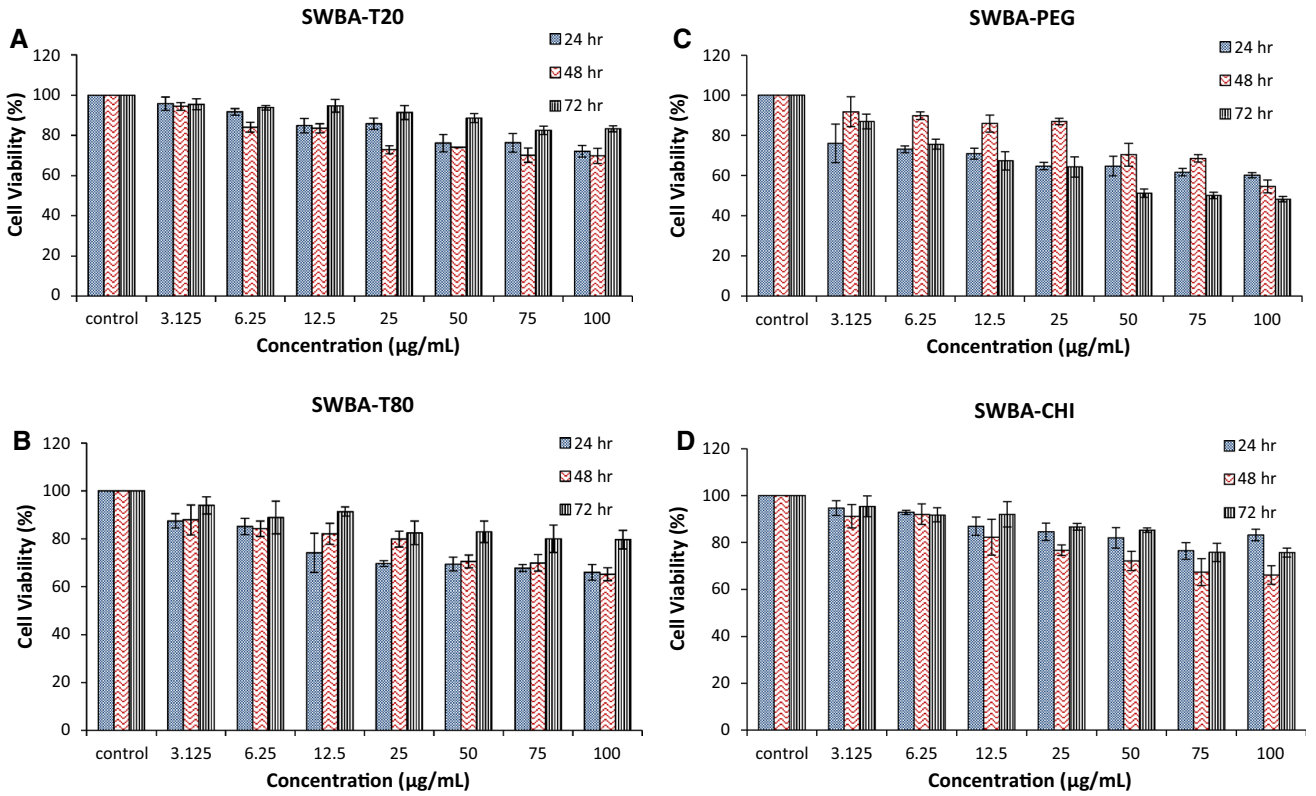

Fig. 8 In vitro cell viability of 3T3 cells treated with **a** SWBA-T20, **b** SWBA-T80, **c** SWBA-PEG, and **d** SWBA-CHI at different concentrations for 24, 48 and 72 h. *Error bars* represent mean ± SD for $n = 3$

acids, catalyst residue, heavy metals, etc.) and by-product (e.g., 1,4-dioxane) found in PEG [46] should also be taken into consideration.

The MTT assay on 3T3 cells shows a continuing growth in cell numbers after exposure to SWBA-T20, SWBA-T80, and SWBA-CHI at 72 h. This observation is in line with the slow and sustained release pattern of BA coated by T20, T80, and CHI, with a maximum release of 47, 73, and 61 %, respectively. In the case of SWBA-PEG, the viable cells were decreasing after exposure (3 days), which seem to be an acute response to the drug release pattern. This result could be attributed to the fast and rapid drug release of BA from SWBA-PEG due to its high solubility in aqueous environment, with a maximum release of 96 % achieved at day 3. Therefore, we can conclude that the cytotoxicity is dependent upon the surface coating agents as well as the drug release profiles.

4 Conclusions

In summary, we have developed a drug delivery system for the anti-cancer drug, BA based on carboxylated SWCNT in the presence of four biocompatible coating agents. The coatings were confirmed by the FTIR studies, which showed the presence of the agents' important characteristic peaks in the biopolymer-coated SWBA samples. Raman studies revealed that the I_D/I_G ratio of all coated samples decreased significantly after the coating process with the lowest value observed for SWBA-T80, suggesting that T80 has the best surface coverage on SWBA. HR TEM and FESEM studies demonstrated the internal structure and surface morphology of the synthesized SWBA nanocomposites. The drug release experiments showed that the initial burst of BA was dramatically improved with the addition of the surface coating agents and the release rate in pH 7.4 followed the order of SWBA-PEG > SWBA-T80 > SWBA-CHI > SWBA-T20. The release of BA from biopolymer-coated nanocomposites followed the pseudo-second order, suggesting the release was driven by the ion exchange process between the drug molecules and the release medium. The TGA results indicated that the polymer content of T20, T80, PEG, and CHI was calculated to be around 19.3, 56.4, 15.7, and 4.6 wt%, respectively. Finally, we evaluated the cytotoxicity of the biopolymer-coated samples in cell proliferation assay and found that the surface coating agents significantly reduced the cytotoxic effect of the uncoated SWBA. However, further investigations are required in order to optimize the performance and testing of these materials in in vivo models.

Acknowledgments This study is financially supported by the Ministry of Education of Malaysia (MOE) under the PUTRA-IPB grant No. GP-IPB/2013/9425800. Author Julia M. Tan is also grateful to MOE for providing MyPhD scholarship under the MyBrain15 program.

Compliance with ethical standards

Conflicts of Interest The authors declare no conflict of interest.

References

1. Tan JM, Arulselvan P, Fakurazi S, Ithnin H, Hussein MZ. A review on characterizations and biocompatibility of functionalized carbon nanotubes in drug delivery design. J Nanomater. 2014;. doi:10.1155/2014/917024.
2. Zheng X, Wang T, Jiang H, Li Y, Jiang T, Zhang J, Wang S. Incorporation of carvedilol into PAMAM-functionalized MWNTs as a sustained drug delivery system for enhanced dissolution and drug-loading capacity. Asian J Pharm Sci. 2013;8:278–86.
3. Gaillard C, Duval M, Dumortier H, Bianco AJ. Carbon nanotube-coupled cell adhesion peptides are non-immunogenic: a promising step toward new biomedical devices. Pept Sci. 2011;17:139–42.
4. Huang H, Yuan Q, Shah JS, Misra RDK. A new family of folate-decorated and carbon nanotube-mediated drug delivery system: synthesis and drug delivery response. Adv Drug Deliv Rev. 2011;63:1332–9.
5. Kostarelos K, Lacerda L, Pastorin G, et al. Cellular uptake of functionalized carbon nanotubes is independent of functional group and cell type. Nat Nanotechnol. 2007;2:108–13.
6. Jos A, Pichardo S, Puerto M, Sánchez E, Grilo A, Cameán AM. Cytotoxicity of carboxylic acid functionalized single wall carbon nanotubes on the human intestinal cell line Caco-2. Toxicol Vitro. 2009;23:1491–6.
7. Saxena RK, Williams W, Mcgee JK, Daniels MJ, Boykin E, Gilmour MI. Enhanced in vitro and in vivo toxicity of polydispersed acid-functionalized single-wall carbon nanotubes. Nanotoxicology. 2007;1:291–300.
8. Rastogi R, Kaushal R, Tripathi SK, Sharma AL, Kaur I, Bharadwaj LM. Comparative study of carbon nanotube dispersion using surfactants. J Colloid Interf Sci. 2008;328:421–8.
9. Berlin JM, Leonard AD, Pham TT, et al. Effective drug delivery, in vitro and in vivo, by carbon-based nanovectors noncovalently loaded with unmodified paclitaxel. ACS Nano. 2010;4:4621–36.
10. Tan JM, Karthivashan G, Arulselvan P, Fakurazi S, Hussein MZ. Sustained release and cytotoxicity evaluation of carbon nanotube-mediated drug delivery system for betulinic acid. J Nanomater. 2014;. doi:10.1155/2014/862148.
11. Magrez A, Kasas S, Salicio V, Pasquier N, Seo JW, Celio M, Catsicas S, Schwaller B, Forró L. Cellular toxicity of carbon-based nanomaterials. Nano Lett. 2006;6(6):1121–5.
12. Patočka J. Biologically active pentacyclic triterpenes and their current medicine signification. J Appl Biomed. 2003;10(3):7–12.
13. Sahoo RK, Biswas N, Guha A, Sahoo N, Kuotsu K. Nonionic surfactant vesicles in ocular delivery: innovative approaches and perspectives. Biomed Res Int. 2014;. doi:10.1155/2014/263604.
14. Kaur P, Shin MS, Joshi A, Kaur N, Sharma N, Park JS, Sekhon SS. Interactions between multiwall carbon nanotubes and poly(-diallyl dimethylammonium) chloride: effect of the presence of a surfactant. J Phys Chem B. 2013;117:3161–6.
15. Vinardell MP, Infante MR. The relationship between the chain length of non-ionic surfactants and their hemolytic action on human erythrocytes. Comp Biochem Physiol C. 1999;124:117–20.
16. Kerwin BA. Polysorbates 20 and 80 used in the formulation of protein biotherapeutics: structure and degradation pathways. J Pharm Sci. 2008;97:2924–35.
17. Kadajji VG, Betageri GV. Water soluble polymers for pharmaceutical applications. Polymers. 2011;3:1972–2009.
18. Li C, Yang K, Zhang Y, et al. Highly biocompatible multi-walled carbon nanotube-chitosan nanoparticles hybrids as protein carriers. Acta Biomater. 2011;7:3070–7.
19. Kong Z, Yu M, Cheng K, et al. Incorporation of chitosan nanospheres into thin mineralized collagen coatings for improving the antibacterial effect. Colloids Surf B. 2013;111:536–41.
20. Kura AU, Hussein-Al-Ali SH, Hussein MZ, Fakurazi S. Preparation of tween 80-zn/al-levodopa-layered double hydroxides nanocomposite for drug delivery system. Sci World J. 2014;. doi:10.1155/2014/104246.
21. Dorniani D, Kura AU, Hussein-Al-Ali SH, Hussein MZ, Fakurazi S, Shaari AH, Ahmad Z. Release behavior and toxicity profiles towards leukemia (WEHI-3B) cell lines of 6-mercaptopurine-PEG-coated magnetite nanoparticles delivery system. Sci World J. 2014;. doi:10.1155/2014/972501.
22. Guo Z, Xiong J, Yang M, et al. Dispersion of nano-TiN powder in aqueous media. J Alloy Compd. 2010;493:362–7.
23. Xiong J, Xiong S, Guo Z, Yang M, Chen J. Fan. Ultrasonic dispersion of nano TiC powders aided by tween 80 addition. Ceram Int. 2012;38:1815–21.
24. Borges AC, Jayakrishnan A, Bourban PE, Plummer CJG, Pioletti DP, Månson JAE. Synthesis and photopolymerization of tween 20 methacrylate/N-vinyl-2-pyrrolidone blends. Mater Sci Eng C. 2012;32:2235–41.
25. Shameli K, Ahmad M, Jazayer SD, et al. Synthesis and characterization of polyethylene glycol mediated silver nanoparticles by the green method. Int J Mol Sci. 2012;13:6639–50.
26. Xu XH, Ren GL, Cheng J, Liu Q, Li DGJ. Layer by layer self-assembly immobilization of glucose oxidase onto chitosan-graft-polyaniline polymers. Mater Sci. 2006;41:3147–9.
27. Ge B, Tan Y, Xie Q, Ma M, Yao S. Preparation of chitosan-dopamine-multiwalled carbon nanotubes nanocomposite for electrocatalytic oxidation and sensitive electroanalysis of NADH. Sensors Actuator B. 2009;137:547–54.
28. Liu AH, Honma I, Zhou HS. Electrochemical biosensor based on protein-polysaccharide hybrid for selective detection of nanomolar dopamine metabolite of 3,4-dihydroxiphenylacetic acid (DOPAC). Eletrochem Commun. 2005;7:233–6.
29. Lei XW, Ni QQ, Shi JX, Natsuki T. Radial breathing mode of carbon nanotubes subjected to axial pressure. Nanoscale Res Lett. 2011;6:492–7.
30. Bokobza L, Zhang J. Raman spectroscopic characterization of multiwall carbon nanotubes and of composites. Exp Polym Lett. 2012;6:601–8.
31. Ponnamma D, Sung SH, Hong JS, Ahn KH, Varughese KT, Thomas S. Influence of non-covalent functionalization of carbon nanotubes on the rheological behavior of natural rubber latex nanocomposites. Eur Polym J. 2014;53:147–59.
32. Nowacki M, Wiśniewski M, Werengowska-Ciećwierz K, et al. New application of carbon nanotubes in haemostatic dressing filled with anticancer substance. Biomed Pharmacother. 2015;69:349–54.
33. Yeo Y, Park K. Control of encapsulation efficiency and initial burst in polymeric microparticle systems. Arch Pharm Res. 2004;27:1–12.
34. Mehta RC, Thanoo BC, DeLuca PP. Peptide containing microspheres from low molecular weight and hydrophilic poly(d,l-lactide-co-glycolide). J Control Release. 1996;41:249–57.
35. Benyettou F, Hardouin J, Lecouvey M, Jouni H, Mottle L. PEGylated versus non-PEGylated γFe_2O_3@alendronate nanoparticles. J Bioanal Biomed. 2012;4:039–45.

36. Muzzalupo R, Tavano L, Cassano R, Trombino S, Cilea A, Picci N. Colon-specific devices based on methacrylic functionalized tween monomer networks: swelling studies and in vitro drug release. Eur Polym J. 2010;46:209–16.
37. Muzzarelli R, Baldassarre V, Conti F, Ferrara P, Biagini G, Gazzanelli G, Vasi V. Biological activity of chitosan: ultrastructural study. Biomaterials. 1988;9:247–52.
38. Mehta SK, Kaur G, Bhasin KK. Tween-embedded microemulsions—physicochemical and spectroscopic analysis for antitubercular drugs. AAPS PharmSciTech. 2010;11(1):143–53.
39. Hussein-Al-Ali SH, Arulselvan P, Fakurazi S, Hussein MZ. The in vitro therapeutic activity of betulinic acid nanocomposite on breast cancer cells (MCF-7) and normal fibroblast cell (3T3). J Mater Sci. 2014;49:8171–82.
40. Ratanajiajaroen P, Watthanaphanit A, Tamura H, Tokura S, Rujiravanit R. Release characteristic and stability of curcumin incorporated in β–chitin non-woven fibrous sheet using tween 20 as an emulsifier. Eur Polym J. 2012;48:512–23.
41. Ho YS, McKay G. A comparison of chemisorption kinetic models applied to pollutant removal on various sorbents. Process Saf Environ. 1998;76:332–40.
42. Ren W, Tian G, Jian S, et al. TWEEN coated $NaYF_4$: Yb, Er/$NaYF_4$ core/shell upconversion nanoparticles for bioimaging and drug delivery. RSC Adv. 2012;2:7037–41.
43. Hu X, Wang Y, Peng B. Chitosan-capped mesoporous silica nanoparticles as pH-responsive nanocarriers for controlled drug release. Chem Asian J. 2014;9:319–27.
44. Herold DA, Rodeheaver GT, Bellamy WT, Fitton LA, Bruns DE, Edlich RF. Toxicity of topical polyethylene glycol. Toxicol Appl Pharm. 1982;65:329–35.
45. Beasley VR, Buck WB. Acute ethylene glycol toxicosis: a review. Vet Human Toxicol. 1980;22:255–63.
46. Fruijtier-Pölloth C. Safety assessment on polyethylene glycols (PEGs) and their derivatives as used in cosmetic products. Toxicology. 2005;214:1–38.